Journal of Coastal Research	24	4C	141–149	West Palm Beach, Florida	July 2008

Modeling the Effects of Wave Skewness and Beach Cusps on Littoral Sand Transport

Kevin A. Haas†, Lindsay A. Check‡, and Daniel M. Hanes§

†Georgia Tech Savannah
210 Technology Circle
Savannah, GA 31407, U.S.A.
kevin.haas@gtsav.gatech.edu

‡Envirodesign, Inc.
153 Northeast Cove Road
Dawsonville, GA 30534, U.S.A.
lcheck@envirodesign.com

§Coastal and Marine Geology Program
U.S. Geological Survey
400 Natural Bridges Drive
Santa Cruz, CA 95060, U.S.A
dhanes@usgs.gov

ABSTRACT

HAAS, K.A.; CHECK, L.A., and HANES, D.M., 2008. Modeling the effects of wave skewness and beach cusps on littoral sand transport. *Journal of Coastal Research,* 24(4C), 141–149. West Palm Beach (Florida), ISSN 0749-0208.

A process-based numerical modeling system is utilized for predicting littoral sand transport. The intent is to examine conditions slightly more complex than linear waves impinging upon a plane beach. Two factors that we examine are wave skewness and longshore varying bathymetry. An empirical model is used for calculating the skewed bottom wave orbital velocity. The advection of sediment due to the skewed wave velocity is larger and in the direction of the waves, opposite to the results with sinusoidal wave velocities, due to the increase in the bottom shear stress under the wave crests. The model system is also applied to bathymetry containing beach cusps. When the wave field has relatively weak longshore wave power, the currents and the littoral transport exhibit significant longshore variability, thereby altering the overall mean littoral transport.

ADDITIONAL INDEX WORDS: *Littoral transport, wave skewness, beach cusps.*

INTRODUCTION AND MOTIVATION

Littoral sediment transport is of importance to developers, engineers, researchers, and landowners because of the impact of the transport on beach morphology and shoreline evolution. The dominant mechanism for littoral sediment transport is the combination of broken waves and wave-generated longshore currents in the surf zone. Evidence of longshore sediment transport is usually quite pronounced at inlet structures as often seen by deposition and erosion on opposite sides of the inlet. Longshore transport will typically change directions and magnitude seasonally or on even shorter time scales such as during storm events. The design of coastal structures, dredging plans, and sand transfer facilities relies on accurate predictions of longshore sediment transport.

The simplest methods for computing total littoral sand transport are empirical equations developed from scores of data. A commonly used predictive formula was presented by KOMAR and INMAN (1970) and is also referred to as the CERC formula. This formula relates immersed weight sediment transport rate, I_l, to the longshore component of wave energy flux, P_l, at the breakpoint:

$$I_l = KP_l \tag{1}$$

where

$$P_l = (ECn \cos\alpha \sin\alpha)_b, \tag{2}$$

C is the wave celerity, n is the ratio of wave group speed to wave celerity, a is the wave angle relative to shore normal, and K is an empirical coefficient of order (1). E is the wave energy density given by

$$E = \frac{1}{8}\rho g H^2 \tag{3}$$

where H is the root-mean-square wave height. In this formula the wave forcing is characterized by a single height, direction, and breakpoint, and all quantities are evaluated at the breakpoint. Throughout the remainder of this article, the subscript b will denote the quantity at the breakpoint, defined as the cross-shore location with maximum wave height.

The immersed-weight sediment transport is related to the volumetric sediment transport rate (Q_l) as follows:

$$Q_l = \frac{I_l}{\rho(s-1)g(1-p)} \tag{4}$$

where s is the specific gravity of the sediment, and p is the sediment porosity.

KAMPHUIS (1990) suggested an alternate predictive formula for longshore sediment transport based upon dimensional analysis and calibration using laboratory data. The Kamphuis formulation for total sediment transport rate is:

$$Q_l = \left[\frac{\rho H^3}{T} 0.0013(\tan\beta)^{0.75}\left(\frac{H}{\lambda_\infty}\right)^{-1.25}\left(\frac{H}{D_{50}}\right)^{0.25}\sin^{0.6}(2\alpha)\right]_b \tag{5}$$

where D_{50} is the median grain size, T is the peak wave period, $\tan\beta$ is the beach slope, and λ_α is the deep-water wavelength.

A third formula for longshore sediment transport is contained within the GENESIS model (U.S. ARMY CORPS OF ENGINEERS, 2001). The model calculates shoreline evolution re-

DOI: 10.2112/06-0759.1 received 18 September 2006; accepted in revision 8 May 2007.

sulting from spatial and temporal gradients in longshore sediment transport. The predictive formula for longshore sediment transport in GENESIS is:

$$Q_l = \left[H^2Cn\left(a_1\sin 2\alpha - a_2\cos\alpha\frac{dH}{dy}\right)\right]_b. \tag{6}$$

The nondimensional parameters a_1 and a_2 are:

$$a_1 = \frac{K_1}{16\left(\frac{\rho_s}{\rho} - 1\right)(1 - p)} \quad \text{and} \tag{7}$$

$$a_2 = \frac{K_2}{8\left(\frac{\rho_s}{\rho} - 1\right)(1 - p)\tan\beta} \tag{8}$$

where K_1 and K_2 are empirical coefficients. If K_1 is equal to K and the longshore gradient in wave height is zero, the GENESIS equation is the same as the CERC equation shown in Equation (1). The second term in Equation (6) is intended to account for strong alongshore variations in breaking wave height.

The goal in the present work is to utilize process-based numerical models to simulate longshore sediment transport to examine the effects of various processes on littoral transport. Haas and Hanes (2004) used a process-based model to predict the longshore sediment transport on a plane beach subjected to linear monochromatic waves. They found that the total predicted longshore sediment flux was consistent with Equation (1), and they went on to utilize the model to investigate the effects of the cross-shore beach profile and the sediment size upon the total longshore sediment transport. Here we seek to expand the previous work by including increasingly more realistic wave and beach morphology characterization. Specifically, we are including the effect of wave velocity skewness in the calculation of the local sediment transport to examine the effect on the littoral transport. In addition, we run simulations for cusped beach geometries with a random wave field to examine the differences in the longshore sediment transport due to beach cusps.

MODELING APPROACH

The Nearshore Community Model (NearCoM) provides the framework for the connection of wave modules, circulation modules, and sediment transport modules. In this work we use the REF/DIF-1 or REF/DIF-S models for waves (Kirby and Dalrymple 1994; Kirby and Ozkan 1994) accounting for the combined effects of bottom-induced refraction–diffraction, current-induced refraction, and wave-breaking dissipation. The SHORECIRC model is utilized for simulating the circulation (Svendsen *et al.,* 2002). The model determines the flow pattern by solving the quasi-3-D short-wave–averaged hydrodynamic equations for the depth-integrated flow properties. The depth variations of the mean currents are found by solving the local (depth-varying) momentum equations utilizing a perturbation expansion assuming that the radiation stress and bottom stress are the dominate forcing terms for the depth variations, resulting in a polynomial expression for the currents. The sediment transport module uses several alternative total sediment transport formulations: a generic sediment transport developed by Haas and Hanes (2004) (HH), Bowen (1980) (BBB), and Watanabe (1992) (W).

The Haas and Hanes (2004) local longshore sediment transport formula characterizes the total sediment flux by the product of the mobilization due to bed shear stress and the advection due to the total velocity. The HH formula is based on the assumption that

$$\vec{q}_{HH} \propto \overline{|\vec{u}|^2\vec{u}} \propto \overline{|\vec{\tau}|\vec{u}}, \tag{9}$$

with $\vec{u}(t) = \vec{u}_w(t) + \vec{V}(t)$, and $\vec{u}_w$ is the near bottom wave orbital velocity, $\vec{V}$ is the near bottom mean (averaged for the short wave period) current velocity, and the overbar represents the time-averaging during a short wave period.

If the magnitude of the shear stress on the seabed is written as:

$$|\vec{\tau}| = \frac{1}{2}\rho f_w|\vec{u}|^2 \tag{10}$$

where f_w is the wave friction factor, and the effective shear stress which accounts for the initiation of sedimentation is given by:

$$\tau_{eff} = |\vec{\tau}| - \tau_{cr} \tag{11}$$

where τ_{cr} is the critical shear stress, then the local time averaged longshore sediment transport equation as shown in Haas and Hanes (2004) is written as:

$$\overline{q_{HH,y}} = \frac{2C_1}{\rho g}(\overline{\tau_{eff}u_{wy}} + \overline{\tau_{eff}}V_y) \tag{12}$$

where C_1 is a constant. The $\overline{\tau_{eff}u_{wy}}$ represents the advection due to waves, and the $\overline{\tau_{eff}}V_y$ term represents the advection due to the mean current. The critical shear stress is calculated using

$$\tau_{cr} = \rho(s - 1)gD_{50}\theta_{cr} \tag{13}$$

where θ_{cr} is the critical shields parameter for the threshold for incipient motion given as 0.05.

Bagnold (1966) used an energetics approach to develop a predictive formula for bedload and suspended load sediment transport for unidirectional and steady flows. Bowen (1980) and Bailard (1981) modified Bagnold's formulas for directionally and temporally varying flows typical of the nearshore region. The local immersed weight sediment transport rate in the longshore direction using Bowen(1980) is:

$$i_y = \frac{\varepsilon_s(1 - \varepsilon_b)\rho f}{W_o}\overline{|\vec{u}|^3u_y} + \frac{\varepsilon_b\rho f}{\tan\phi}\overline{|\vec{u}|^2u_y} \tag{14}$$

where W_0 is the sediment fall velocity, u_y is the longshore component of the instantaneous total bottom velocity, ε_s is the suspended load efficiency factor, ε_b is the bedload efficiency factor, and tan ϕ is the internal friction angle. The volumetric sediment transport rate can then be found by using the conversion factor in Equation (4).

WATANABE (1992) (W) based a longshore sediment transport equation on energy dissipation as shown by:

$$q_y = A_c \frac{|\tau_b^{\max} - \tau_{cr}|}{\rho g} V_y \tag{15}$$

where A_c is a constant set at 2.0, $\tau_b^{\max}$ is the maximum instantaneous bottom shear stress from wave and current combined flow, and τ_{cr} is the critical bottom shear stress.

All of the preceding formulations for sediment transport include wave orbital velocities and are sensitive to the method for computing these velocities. In particular, the velocity skewness, which is a measure of the asymmetry of the orbital velocity and is a function of the shape of a wave, is vitally important. Skewness is defined for a set of points Y by:

$$\text{skewness} = \frac{\sum_{i=1}^{N} (Y_i - \bar{Y})^3}{(N-1)s^3} \tag{16}$$

where $\bar{Y}$ is the mean of Y, s is the standard deviation of Y, and N is the number of data points. Skewness is important to sediment transport because as seen in the transport equations above, the transport is proportional to the cube of the velocity. The previous work by HAAS and HANES (2004) used linear theory to compute the wave velocity time series, which results in a skewness value of zero. Therefore, an alternative method is required to compute time series of wave velocities with nonzero skewness values.

Several methods have been developed to calculate the skewed orbital velocities typical of surface gravity waves in shallow water. ELGAR and GUZA (1986) used Boussinesq equations to calculate skewness of shoaling waves. DOERING and BOWEN (1995) used an empirical calculation from bispectral analysis to find velocity skewness of cross-shore flow. Stream function wave theory was developed by DEAN (1965) to provide a representation of a nonlinear gravity water wave. The aforementioned methods were not chosen in the present research because of excessive computation time or limited applicability in the nearshore region, particularly in the surf zone.

Nearbed velocity time series for skewed waves are calculated using the method by ELFRINK *et al.* (2006). The method describes the time variation of nearbed orbital velocities of individual waves in irregular wave trains. These expressions for velocity skewness and velocity time series under shoaling and breaking waves were derived using data mining and evolutionary algorithms to fit field measurements that were mainly collected at Terschelling, The Netherlands, and Duck, North Carolina.

Suite of Tests

Tests are performed on idealized typical beach profiles and also on barred and cusped beach morphologies. The typical profile, which we will refer to as the average beach profile (ABP) is:

$$h = Ax_h^n \tag{17}$$

where x_h is the distance from the shoreline with offshore being positive, A = 0.1 ($m^{1/3}$) for a sediment diameter of 0.2 mm, and n is ALERT2/3.

When an input parameter or case is changed, a suite of tests is run for the case. The suite includes the combination of deep-water root-mean-square wave heights of 0.1, 0.25, 0.5, 1.0, 1.5, 2.0, 2.5, and 3.0 m and deep-water wave angles of 3°, 6°, 9°, 12°, and 15°. The peak wave period for the smaller wave heights of 0.10 m and 0.25 m is 4 seconds and for wave heights from 0.5 m to 3 m is 10 seconds.

The variability of wave height and wave angle provides a large range of P_l, which enables a thorough comparison with established laboratory measurements, field data, and empirical formula predictions. Input parameter and case changes include wave driver type, grain size, bathymetric variability, velocity skewness, transport skewness, and longshore sediment transport formula. Wind and tidal effects are not considered.

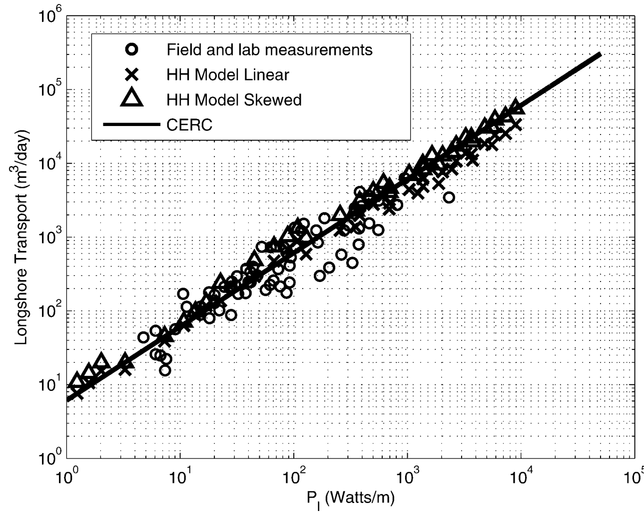

Figure 1. Total longshore transport for linear and skewed wave cases. Just for reference, results are compared to the CERC formula and field and laboratory measurements.

EFFECTS OF WAVE ORBITAL VELOCITY SKEWNESS

The time-averaged longshore sediment flux is calculated as a function of cross-shore position using the different formulations (*i.e.,* HH, BBB, and W) and is integrated across the surf zone to produce total longshore sediment transport. The inclusion of skewed orbital velocities in the bottom shear stress and transport calculations has an impact on the resulting sediment transport. Figure 1 shows the total longshore sediment transport as a function of the longshore wave power predicted by the HH formula (C_1 = 2.0) for the linear and skewed wave cases and includes the CERC formula re-

Table 1. *Best fit parameters for transport formulas HH, BBB, and W for linear and skewed cases where* N *is the exponent and* K *is the coefficient from Equation (21).* K_f *is the coefficient for the best fit while holding* N *constant with a value of one.*

Formula	Case	N	K	K_f	Variance	% Change of K_f
HH	Linear	0.92	0.84	0.54	0.088	—
HH	Skewed	0.96	1.06	0.84	0.048	55%
BBB	Linear	1.02	0.48	0.54	0.020	—
BBB	Skewed	1.05	0.63	0.86	0.079	57%
W	Linear	0.95	3.18	2.54	0.027	—
W	Skewed	0.78	2.91	2.91	0.29	15%

sults for comparison. The same coefficient is used for both the linear and skewed case to make it clear from Figure 1 that including the skewed orbital velocities increases the total longshore transport. A conclusion that the skewed waves match the CERC formula more closely would be erroneous because a different choice for the coefficient could easily enable the linear waves to match the CERC formula.

A best-fit line to the model output is found by combining Equations (1) and (4) and fitting the equation

$$I = Q_l \rho(s - 1)g(1 - p) = KP_l^N \tag{18}$$

to the model data in a least squares sense to find optimal values of K and N. For the log-log plots, the power N corresponds to the slope of the best fit line for the model output. Alternatively, N can be fixed at 1.0 similar to the CERC formula, and a ratio R can be defined as:

$$R = \frac{K_f P_l}{I} \tag{19}$$

where I is the immersed weight transport, and P_l is the longshore wave power, both computed from the model. K_f is found by minimizing the deviations of this ratio from a value of 1.0 for each wave condition from the model runs in a least squares sense. Variations in K_f values are a direct indicator of relative differences in total longshore transport for each formula, where larger values of K_f indicate more longshore transport. The value of the variance (R) is indicative of the scatter of the model output from this best fit line.

The properties of the best fit lines from the model results are shown in Table 1. The value of N in Table 1 provides a measure of the proximity of the model results to the CERC formula power of 1.0 using various local sediment transport formula predictions (HH, BBB, and W). Table 1 shows that the total transport for each sediment transport equation predicts higher total sediment transport for the skewed cases. The addition of the skewed velocities in the shear stress and transport calculations increases the K_f value for HH by 55%, BBB by 57%, and W by 15%. The magnitude of increase in longshore sediment transport highlights the importance of accounting for higher-order terms affecting the wave shape. The variance is smallest for the linear BBB cases and is the highest for the skewed Watanabe cases. There is an increase in variance for the skewed cases over the linear cases for each formula except HH.

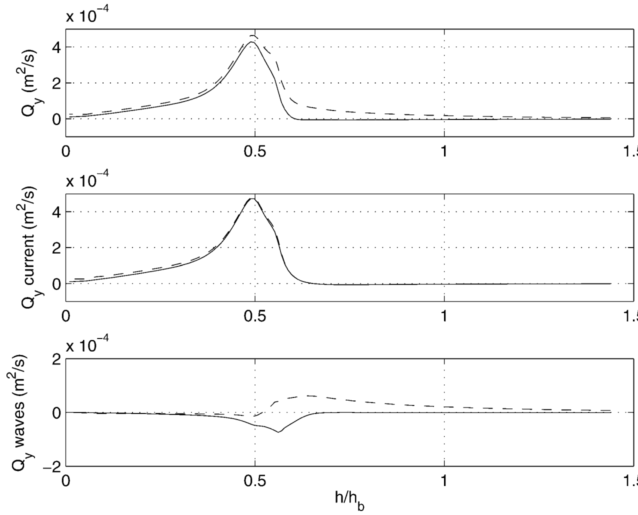

Figure 2. Longshore sediment volume flux (top panel), longshore volume flux due to current (middle panel), and longshore sediment volume flux due to waves (bottom panel). Solid lines are for linear waves, and dashed lines are for the skewed waves.

In order to explain the overall increase in longshore sediment transport due to skewed waves, we examine the details from simulations with and without wave skewness from one particular wave condition corresponding to a deep-water wave height of 1.5 m, a deep-water wave angle of 6°, and with the HH local sediment transport formula. The cross-shore distribution of the longshore sediment volume flux is shown in the upper panel of Figure 2. The middle and lower panels show the breakdown of the contributions to longshore transport due to advection by the current (second term in the brackets of Equation [12]) and due to advection by the waves (first term in the brackets of Equation [12]). Sediment transport because of advection by the longshore current is always positive (in the direction of the longshore current) for both linear and skewed waves. However, the flux due to waves is negative for the linear waves and positive for the skewed waves. Although the wave-induced transport is negative for the linear case, the total transport remains positive because the transport due to the current is much larger in magnitude. The reason that the flux due to waves is not zero for the linear case is that the transport is defined as the product of the bottom shear stress (due to the combined wave and current flow) with the wave velocity. Therefore this transport component has terms proportional to the wave velocity squared as well as cubed.

The explanation of the negative longshore sediment transport contribution by the wave advection term for the linear wave case is related to the interplay between the orbital velocity and the mean velocity (undertow and longshore currents) in determining the bed shear stress. Figures 3 and 4, respectively, show the effective shear stress for the linear and skewed wave cases. In the case of linear waves, the undertow adds to the seaward velocity under the wave trough but reduces the shoreward velocity under the crest, whereas the

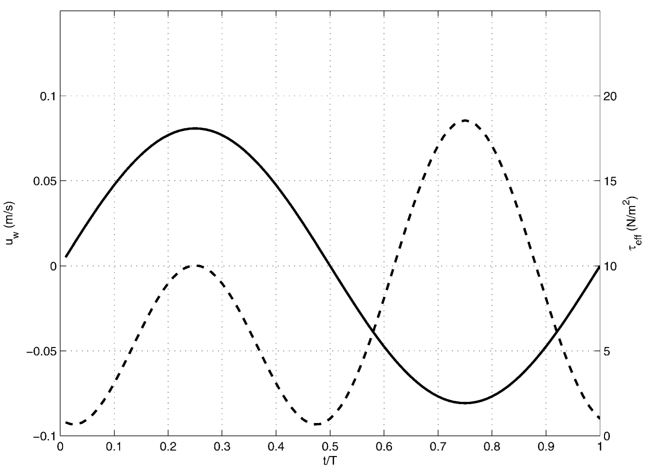

Figure 3. Time-varying orbital velocity (solid line) and the magnitude of the effective shear stress (dashed line) for linear wave case inside the surfzone.

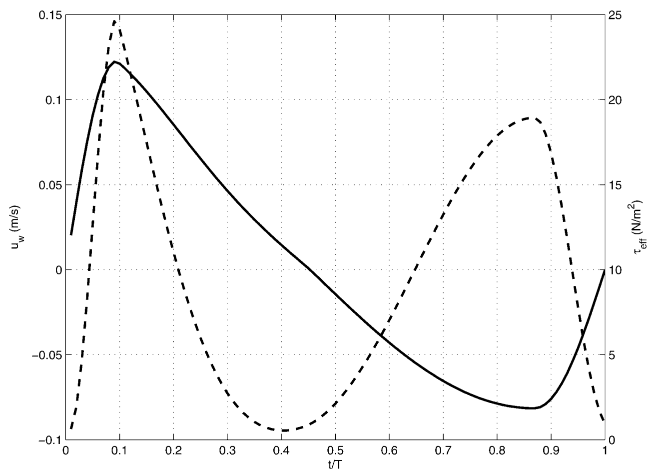

Figure 4. Time-varying orbital velocity (solid line) and the magnitude of the effective shear stress (dashed line) for the skewed wave case inside the surfzone.

longshore current adds to the longshore wave velocity under the crest and decreases the longshore wave velocity under the trough. The relative change in shear stress due to the undertow exceeds the change caused by the longshore current; therefore, the bottom shear stress is greater under the wave trough than it is under the wave crest. The transport direction is governed by the orbital velocity direction, and because the shear stress is larger and the transport direction is offshore under the trough, the net result is a seaward transport of sediment, and an "updrift" longshore sediment transport contribution due to the waves not being normally incident. When the waves are skewed, the enhanced shear stress under the crest due to the wave skewness is sufficient to overcome the contribution of the undertow, so the net transport is in the direction of wave advance, and contributes positively toward the longshore sediment transport. We note, however, that the sediment transport formulation does not include bed slope effects that tend to shift the transport direction offshore and therefore does not contribute to longshore transport under the present conditions.

The effect of the skewed waves increasing the littoral transport is illustrated with the HH sediment transport formulation. However, the basic mechanism causing the increase in transport remains the same regardless of which sediment transport formulation is used. It is worth mentioning that the skewed wave velocity has an even more pronounced effect on the cross-shore sediment transport because with linear waves the transport would all be offshore and no accretion or onshore transport would be possible, which is clearly unrealistic.

Our modeling approach to address the effects of wave skewness on longshore transport makes several assumptions that could be improved upon in the future. Foremost among these assumptions is that the sediment flux is related to the hydrodynamic forcing in an instantaneous manner. Whereas this is likely the case for sheet flow (Hsu and Hanes, 2004), it is not the case for suspended sediment transport under temporally varying wave conditions (Vincent and Hanes, 2002).

MODEL APPLICATION TO A CUSPED BEACH

Bars, cusps, ripples, megaripples, ridges, and sand waves on beaches are all nearshore features that may have an impact on longshore sediment transport and hydrodynamics (Werner and Fink, 1993). A common morphology occurring near the shoreline is beach cusps. We next use the models to examine the effects of beach cusps on longshore sediment transport. For the model runs with the cusped beach bathymetry, the bathymetry is held constant, permitting no erosion or accretion of the shape, but calculating localized transport rates across the bathymetry. We are therefore not addressing the origin or stability of beach cusps. The idealized cusped beach bathymetry is created using the following equation adapted from Rogers *et al.* (2002):

$$h_0 = Ax^n + h_{\min} + \varepsilon \cos ky \exp\left(\frac{-x}{\lambda_c}\right) \tag{20}$$

where $k = 2\pi/L_c$, $h_{\min}$ is the depth at the shoreline, L_c is the longshore cusp length, ε is the cusp amplitude, and λ_c is the cusp offshore decay parameter, which is taken to be 25 m for all tests. The suite of tests performed includes cusp amplitudes of 0.1, 0.25, and 0.5 m and corresponding cusp lengths of 10, 25 and 50 m.

The wave field is computed with Ref/Dif-S simulating a random wave field. The longshore variability in the bathymetry due to the beach cusps creates different regions of wave convergence and divergence. Near the breaker line where the bathymetric variability is fairly weak, there is only a small amount of variability in the wave height. As seen in Figure 5, the wave height and wave angle have weak longshore variations with the waves being slightly larger around y = 12.5 m, which is a region of shallower water depth as seen in the depth contours shown in Figure 6. From the wave angle it is

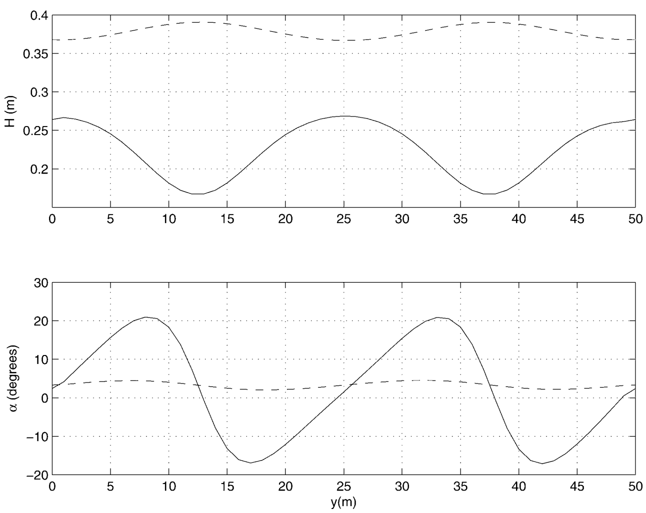

Figure 5. Longshore variability of wave height (top panel) and angle (bottom panel) for $\varepsilon = 0.25$ m, $L_c = 25$ m, $\lambda_c = 25$, $H_b = 0.5$ m near the break line (dashed) and near the shoreline (solid).

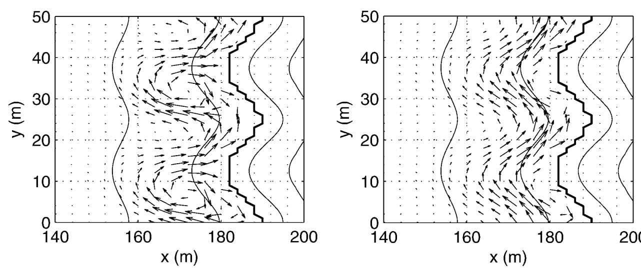

Figure 6. Velocity vectors and bathymetric contours for $\varepsilon = 0.25$ m, $L_c = 25$ m, $\lambda_c = 25$, $H_b = 0.5$ m, and deep-water wave angles $\alpha = 3°$ (left panel) and $\alpha = 9°$ (right panel).

clear that the waves are converging to this region, although fairly weakly.

Within the surfzone close to the shoreline where the bathymetry has strong longshore variations, the wave height and wave angle have much larger longshore variability. There is strong wave focusing onto the horns of the cusps as seen from the wave angle; however, the wave height is actually smaller in this region. This is because with the shallow depth, the wave dissipation due to breaking is much stronger, and therefore the wave heights are fairly small.

As expected, the circulation patterns on a cusped beach are highly sensitive to the incoming wave angle. For small breaking wave angles (under 3°), eddies are formed such as shown in the left panel of Figure 6, which leads to a flow reversal at some longshore locations. With larger breaking wave angles, as seen in the right panel of Figure 6, the flow reversal no longer occurs, although the flow does still have significant longshore variability, because the larger angle generates flow with enough momentum to overcome the adverse pressure gradients generated by the wave focusing.

Longshore sediment transport is calculated on the cusped beach for the full suite of wave conditions as described earlier using the HH sediment transport formula (the other transport models give similar results). Figure 7 shows the cross-shore variation of longshore transport at a variety of longshore positions corresponding to different parts of the cusp bathymetry. The two cases shown correspond to the two cases in Figure 6, deep-water wave height of 0.5 m and deep-water wave angles of 3° and 9°. The first cross-section (y = 12 m) is in the shallowest part of the cusp, whereas the cross-section at y = 24 m is in the deepest part of the cusp. Within the outer part of the surfzone the longshore transport is always positive; however, inside the inner surfzone the transport is actually negative at several longshore positions because of the flow reversals. This trend is reduced significantly for the larger wave angle, with only a small portion of the transport being negative at y = 30 m.

The longshore sediment transport is integrated in the cross-shore direction to obtain the total longshore transport as a function of longshore position. Figure 8 shows the alongshore variation of longshore sediment computed with the HH model. The transport varies strongly in the longshore direction because of the effect of the beach cusps on the wave refraction, wave breaking, and the associated hydrodynamics. The longshore locations of the extremes in longshore transport occur approximately between the crest and trough of the beach cusp, with the maximum being as the flow goes from the cusp crest to trough.

Figure 8 also shows the alongshore variability of the predictions of the total longshore sediment transport by the CERC, Kamphuis, and GENESIS empirical formulas, based upon local conditions at the breakpoint. The cusped beaches present an interesting case for an application of the GENESIS empirical formula for total sediment transport. As seen

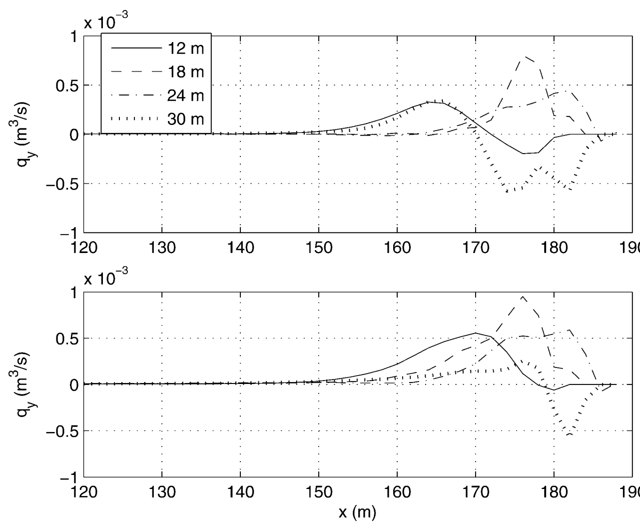

Figure 7. Cross-shore variation of longshore transport along multiple cross sections for $\varepsilon = 0.25$ m, $L_c = 25$ m, $\lambda_c = 25$, $H_b = 0.5$ m, and $\alpha = 3°$ (top panel) and $\alpha = 9°$ (bottom panel). The longshore location of 12 m corresponds to a cusp crest, and 24 m corresponds to a cusp trough.

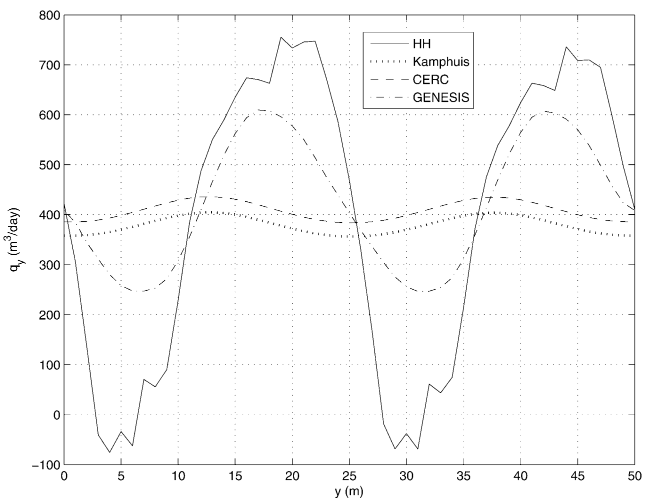

Figure 8. Longshore variability of longshore transport for $\varepsilon = 0.25$ m, $L_c = 25$ m, and $\lambda_c = 25$ m for $H = 0.5$ m and $\alpha = 6°$.

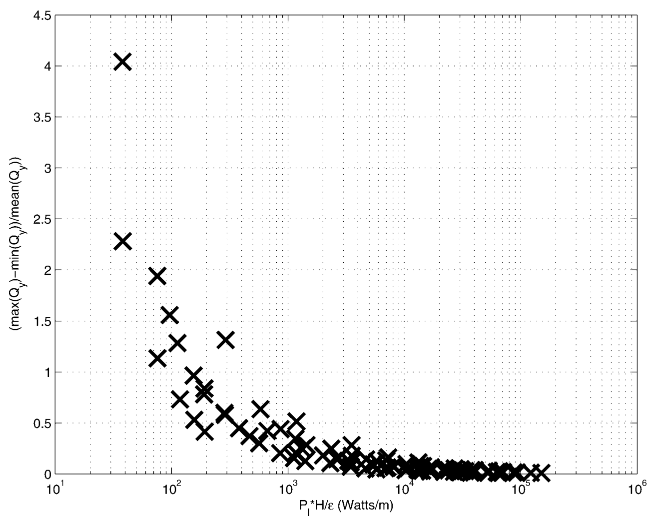

Figure 9. The range in the longshore variation of the cross-shore integrated longshore transport normalized by the mean transport as a function of the product of the longshore wave power and the wave height over cusp amplitude.

in Equation (6), the GENESIS formula includes a term, ALERTdH/dy, which takes into account the longshore gradient of the wave height and is nonzero on a cusped bathymetry. For the longshore uniform beach profiles with longshore uniform forcing, the gradient term is zero because there is no alongshore variation, and therefore the GENESIS formulation matches the CERC formula.

All three formulas show at least some longshore variability, although all are less variable than the HH predictions. The CERC and GENESIS formulas would be equivalent if the longshore gradient in wave height were zero; however, on the cusped beach the gradient term leads to the phase shift in longshore variability seen between the CERC and GENESIS formulas. In addition, the GENESIS formula has much stronger longshore variability than the CERC formula although the longshore mean is similar (around 420 m^3/d), leading to the conclusion that the addition of the wave height gradient term is important to the local transport but not the longshore averaged transport. The Kamphuis and the CERC formulas have very similar longshore variations with just a small difference in overall magnitude. This is because these formulations are only a function of the wave height directly, and therefore the longshore variability only arises because of the variability in the breaking wave height. However, the model and HH formulations include the additional effect of the gradient of the wave height, which can create pressure gradients that will enhance or retard the longshore current and the resultant sediment transport. This difference in longshore variability has significant implications if the longshore transport is used for modeling shoreline evolution; the gradients of the longshore transport are quite different leading to erosion and accretion in different parts of the beach. As a matter of fact, the HH and GENESIS formulae yield initial transport gradients that tend toward eliminating the beach cusps, whereas the CERC and Kamphuis formulae yield initial transport gradients that would lead to migration of the cusps.

As expected, the longshore variability of the total longshore sediment transport is a function of the wave height, wave angle, and relative cusp height. To illustrate this point, the longshore minimum of the cross-shore integrated longshore sediment transport is subtracted from the maximum and then nondimensionalized by the mean total longshore sediment transport. This is plotted in Figure 9 as a function of longshore wave power multiplied by the ratio of the breaking wave height over cusp height. For small values of this modified longshore wave power, corresponding to small angles and small wave to cusp height ratios, the variation is quite large with variations up to four times the mean total longshore transport. However, as the modified longshore wave power increases, the variability in longshore transport drops rapidly toward zero.

Finally, a measure of how the beach cusps affect the total longshore transport is computed by finding the ratio of the mean (averaged in the longshore direction) total littoral transport on the cusped beaches divided by the total littoral transport on uniform beaches for the same deep-water wave conditions. This ratio is plotted as a function of the modified longshore wave power in Figure 10. For smaller values of the longshore wave power the ratio is less than one, which corresponds to a small reduction of transport on cusped beaches relative to uniform beaches. Not surprisingly this ratio is close to one for the larger modified longshore wave power because the effect of the beach cusps on the hydrodynamics is minimized due to the large wave to cusp height ratio and the large longshore wave power. One interpretation of this result is that meandering of the currents created by the presence of the beach cusp is reducing the littoral transport capability of the flow.

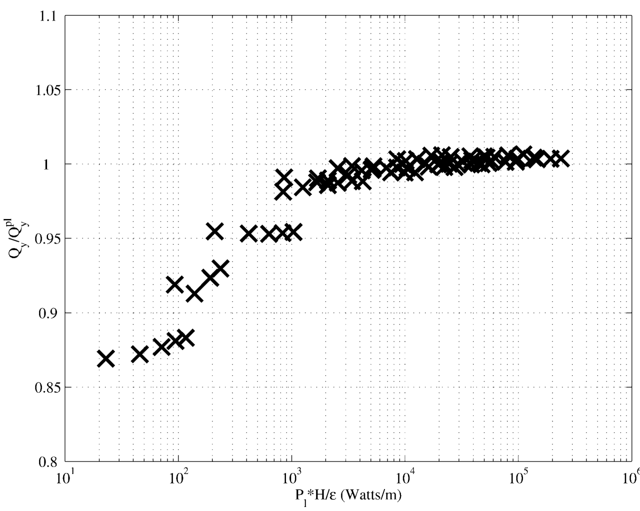

Figure 10. The ratio of the average integrated longshore transport on cusp beaches over the integrated transport on a longshore uniform beach as a function of the product of the longshore wave power and the wave height over cusp amplitude.

CONCLUSIONS

The prediction of longshore sediment transport though the application of a process-based numerical model is desirable for beach nourishment projects, coastal development plans, dredging operations, and additional engineering applications. We have extended the previous work of HAAS and HANES (2004) to evaluate the effects of wave skewness and the effects of beach cusps on the total longshore sediment transport.

An empirical method for determining skewed orbital velocities is incorporated into the model, and the velocities are used in the formulation of the shear stress and transport. It was found that including skewed wave orbital velocities in shear stress and transport calculations increases total longshore sediment transport anywhere from 15% to 56% on average for the full range of conditions tested. However, the increase is larger for the more skewed (larger) waves than for the less skewed (smaller) waves within this range. This increase in transport occurs because the time-varying orbital velocity and effective shear stress under the crest are higher than the linear case. This combination ultimately leads to more longshore sediment transport under the wave crest, which then contributes to a larger overall littoral transport.

Simulations of hydrodynamics and longshore sediment transport were done for random waves on beaches with cusps. Beach cusps cause weak variations in the wave field near the break point and large variations in the inner surfzone. The circulation pattern is altered significantly by the cusp geometry only for cases with relatively small wave angles, which enable eddies or strong deviations in the longshore current to be formed. The resulting longshore transport has longshore variability that is decreasing with increasing wave angles and wave to cusp height ratios. Similarly, the deviation of the longshore transport on cusped beaches as compared to uniform beaches is strongly dependent on the longshore wave power and wave to cusp height ratio. The transport on cusped beaches is reduced for small values of the longshore wave power and wave height to cusp ratio. The longshore variation of the transport computed by the model and with the GENESIS formula are quite similar, whereas the transport computed with the CERC and Kamphuis formulations have similar longshore variability to each other but are quite different from the model and GENESIS variability. Overall the mean longshore transport computed with the process-based transport formulations and the total load formulations are similar, however, because the longshore gradients in the transport are quite different, using the longshore transport to compute shoreline evolution would result in significantly different results.

ACKNOWLEDGMENTS

This work was sponsored by the U.S. Office of Naval Research and the National Science Foundation through the National Oceanographic Partnership Program and the Coastal and Marine Geology Program of the U.S. Geological Survey.

LITERATURE CITED

BAGNOLD, R.A., 1966. An approach to the sediment transport problem from general physics. Professional paper 422-I, U.S. Geological Survey.

BAILARD, J.A., 1981. An energetics total load sediment transport model for a plane sloping beach. *Journal of Geophysical Research,* 86, 10938–10954.

BOWEN, A.J., 1980. Simple models of nearshore sedimentation: Beach profiles and longshore bars. *In*: MCCANN, S.B., *Coastline of Canada.* Halifax, Canada: Geological Survey of Canada, pp.1–11.

DEAN, R., 1965. Stream function representation of non-linear ocean waves. *Journal of Geophysical Research,* 70, 4561–4572.

DOERING, J. and BOWEN, A., 1995. Parameterization of orbital velocity asymmetries of shoaling and breaking waves using bispectral analysis. *Coastal Engineering,* 26, 15–33.

ELFRINK, B.; HANES, D.M., and RUESSINK, G., 2006. Parameterization and simulation of near bed orbital velocities under irregular waves in shallow water. *Coastal Engineering,* 53(11), 915–927.

ELGAR, S. and GUZA, R., 1986. Nonlinear model predictions of bispectra of shoaling surface gravity waves. *Journal of Fluid Mechanics,* 167, 1–18.

HAAS, K.A. and HANES, D., 2004. Process based modeling of total longshore sediment transport. *Journal of Coastal Research,* 20(3), 853–861.

HSU, t.-J. and HANES, D.M., 2004. The effects of wave shape on sheet flow sediment transport, *Journal of Geophysical Research,* 109(C5), C05025, doi: 10.1029/2003JC002075.

KAMPHUIS, J.W., 1990. Littoral sediment transport rate. *In: Proceedings of the 22nd Coastal Engineering Conference, American Society of Civil Engineers* (Delft, the Netherlands, American Society of Civil Engineering), 83(WW1), pp. 1–37.

KIRBY, J.T. and DALRYMPLE, R.A., 1994. REF/DIF 1 combined refraction/diffraction model. Documentation and Users Manual, CACR Rep. No. 94-22. Newark, Delaware: Department of Civil Engineering, University of Delaware.

KIRBY, J.T. and OZKAN, H.T., 1994. REF/DIF S combined refraction/diffraction model. Documentation and Users Manual, CACR Rep. No. 94022. Newark, Delaware: Department of Civil Engineering, University of Delaware.

KOMAR, P.D. and INMAN, D.L., 1970. Longshore sand transport on beaches. *Journal of Geophysical Research,* 75, 5514–5527.

ROGERS, B.; BORTHWICK, A., and TAYLOR, P., 2002. Godunov-type model of wave-induced nearshore currents at multi-cusped beach in the UKCRF. *In: Proceedings 28th International Conference on Coastal Engineering* (Cardiff, Wales, American Society of Civil Engineering), pp. 1–13.

SVENDSEN, I.; HAAS, K., and ZHAO, Q., 2002. Quasi-3D Nearshore Circulation Model SHORECIRC, CACR Report 2002-01. Newark, Delaware: Center for Applied Coastal Research, University of Delaware.

U.S. ARMY CORPS OF ENGINEERS, WAVE EXPERIMENT STATION, 2001. Coastal Engineering Manual, EC 1110-2-1100 Washington, D.C.: U.S. Government Printing Office.

VINCENT C.E. and HANES, D.M., 2002. The accumulation and decay of nearbed suspended sand concentration due to waves and wave groups. *Continental Shelf Research,* 22, 1987–2000.

WATANABE, A., 1992. Total rate and distribution of longshore sand transport. *23rd ICCE,* 3, Venice: ASCE, pp. 2528–2541.

WERNER, B. and FINK, T., 1993. Beach cusps as self-organized patterns. *Science,* 260, 968–971.